

Window Function for MIMO Radar Beamforming to Mitigate Multipath Clutter

Ryuhei Takahashi, Nobuhiro Suzuki, Hirohisa Tasaki

Information Technology R&D Center, Mitsubishi Electric Corporation, Kanagawa, Japan.

Email: Takahashi.Ryuhei@ab.MitsubishiElectric.co.jp

Abstract— In this paper, a novel window function for MIMO (multiple input multiple output) radar beamforming to mitigate multipath clutter is proposed. The proposed window is derived by modeling a covariance matrix of multipath clutter. The computer simulation result indicates that the proposed window has an integrated sidelobe level ratio of -37.8 dB, which is 7.9 dB lower than that of conventional Hamming-on-Hamming window case while maintaining comparable performance in mismatch loss, beamwidth, and peak sidelobe level ratio.

I. INTRODUCTION

Multiple input multiple output (MIMO) radar enables radar system designers to perform digital transmit and receive beamforming, i.e., MIMO beamforming. This function improves radar performance in terms of target angle accuracy [1] and minimum detectable velocity of ground moving target indicator mode [2] owing to the receiver beamwidth of the MIMO radar being finer than that of the conventional phased array radar. Many studies dealing with MIMO radar applications [1]-[6] explicitly considered the direct path propagation between the radar and object and implicitly ignored multipath propagation where the direction-of-departure (DOD) is not equal to the direction-of-arrival (DOA).

However, in radar applications such as over-the-horizon radar and high-frequency surface wave radar (HFSWR), unwanted echoes due to multipath propagation, i.e., multipath clutter, degrade target detection performance [7][8]. Adaptive multipath clutter mitigation techniques are proposed by exploiting the MIMO radar's observability into all transmit and receive propagation paths [9]-[14].

In the design and analysis of multipath clutter mitigation, the MIMO bidirectional beampattern is useful for evaluating sensitivity to radar echo traveling via the direct path and multipath propagation. It evaluates quiescent beamforming gain of the MIMO radar for all propagation paths given by a combination of DOD and DOA. It is a generalization of what is called the "2-way beampattern" [3], which explicitly assumes direct path propagation where DOD is equal to DOA. The MIMO bidirectional beampattern is mapped onto the DOD-DOA plane and the 2-way beampattern appears on the diagonal slice of the pattern where DOD equals DOA.

The MIMO bidirectional beampattern has a higher sidelobe level region along the vertical and horizontal axes associated with the main beam region. This higher sidelobe region is unobservable with the 2-way beampattern. The region corresponds to the DOD and DOA combination where the DOD is within the main beam of the transmit beam and the DOA is within the sidelobe of the receive beam, and vice versa. To refer to the sidelobe region, the term "MS/SM (Main beam-Sidelobe)/(Sidelobe-Main beam)" is used in the following discussion.

Owing to the higher sidelobe level, the MS/SM multipath clutter or target potentially causes false alarm detections, thus leading to detrimental radar performance. To avoid performance degradation due to MS/SM multipath clutter, a novel window function for MIMO radar beamforming is proposed in this paper. The proposed window is derived by modeling the covariance matrix of the MS/SM multipath clutter. The proposed window can be predesigned so that it can be affordably implemented in the MIMO beamforming processor in a non-adaptive manner. Thus, it can be used with adaptive MIMO beamforming methods stated in previous studies [9]-[14].

II. MIMO BIDIRECTIONAL BEAMPATTERN

By defining the transmit steering vector as $\mathbf{a}_T(u_T)$, where u_T is the direction cosine of DOD, and the receive steering vector as $\mathbf{a}_R(u_R)$, where u_R is the direction cosine of DOA, MIMO steering vector is given as

$$\mathbf{a}(u_T, u_R) = \mathbf{a}_T(u_T) \otimes \mathbf{a}_R(u_R), \quad (1)$$

$$\mathbf{a}_T(u_T) = \left[\exp(jku_T d_1^{(TX)}) \quad \cdots \quad \exp(jku_T d_{M_T}^{(TX)}) \right]^T, \quad (2)$$

$$\mathbf{a}_R(u_R) = \left[\exp(jku_R d_1^{(RX)}) \quad \cdots \quad \exp(jku_R d_{M_R}^{(RX)}) \right]^T, \quad (3)$$

where k is wavenumber, $d_{m_T}^{(TX)}$ is the m_T -th ($m_T = 1, \dots, M_T$) transmit element antenna position and $d_{m_R}^{(RX)}$ is the m_R -th ($m_R = 1, \dots, M_R$) receive element antenna position.

Without the loss of generality, the MIMO beamforming directed to the array boresight is considered in the following discussion. MIMO beamforming weight is defined as

$$\mathbf{w}_0 = (\mathbf{T}_T \otimes \mathbf{T}_R)(\mathbf{a}_T \otimes \mathbf{a}_R), \quad (4)$$

where $\mathbf{a}_T \equiv \mathbf{a}_T(0)$ and $\mathbf{a}_R \equiv \mathbf{a}_R(0)$ are the transmit and receive steering vectors for the boresight, respectively. \mathbf{T}_T and \mathbf{T}_R are the transmit and receive window matrices, respectively. The window matrix is a diagonal matrix where conventional window function values, e.g., Hamming, are allocated on the diagonal elements.

Thus, the MIMO bidirectional beam response $y(u_T, u_R)$ is given by

$$\begin{aligned} y(u_T, u_R) &= \mathbf{w}_0^H \mathbf{a}(u_T, u_R) \\ &= y_T(u_T) \cdot y_R(u_R), \end{aligned} \quad (5)$$

where $y_T(u_T)$ and $y_R(u_R)$ are the transmit and receive beam responses, respectively, defined as

$$y_T(u_T) = \mathbf{a}_T^H \mathbf{T}_T^H \mathbf{a}_T(u_T) \quad (6)$$

$$y_R(u_R) = \mathbf{a}_R^H \mathbf{T}_R^H \mathbf{a}_R(u_R) \quad (7)$$

Finally, the MIMO bidirectional beampattern $B(u_T, u_R)$ is described as

$$B(u_T, u_R) = |y_T(u_T)|^2 |y_R(u_R)|^2 \quad (8)$$

Eq. (8) indicates that the bidirectional beampattern is the product of the transmit beampattern and the receive beampattern. As u_T and u_R are independent variables, the bidirectional beampattern can be only evaluated on the two-dimensional DOD–DOA plane. Fig. 1(a) is representative MIMO bidirectional beampattern of 15-MHz HF-MIMO radar where a 32-element uniform linear array (ULA) is used for the transmission and reception and the main beam is steered at the boresight. Two-way beampattern corresponding to the direct path appears toward the diagonal slice thereby satisfying the condition $u_T = u_R$ on the bidirectional beampattern. The bidirectional beampattern has the higher sidelobe level region along the horizontal and vertical axes associated with the main beam corresponding to the MS and SM propagation paths; this higher sidelobe region is unobservable with the 2-way beampattern.

It is noteworthy that the bidirectional beampattern of the MIMO radar with a sparse arrangement of the transmit antenna shows grating lobes for the multipath propagation paths. Fig. 1(b) is the representative bidirectional beampattern of the 15-MHz HF-MIMO radar with sparse transmit array where the two transmit element antenna is located at both ends of the 32 receive element ULA. It is observed that there are grating lobes in the vertical DOD axis associated with the main beam. This indicates that the radar echo, which is reflected at the grating lobe direction of the DOD and arrives at the receive main beam direction potentially raises a false alarm. The 2-way beampattern appearing on the diagonal slice corresponding to the direct path has no grating lobes. It can be concluded that the MIMO radar with a sparse array arrangement is unsuitable for use in a strong multipath propagation environment.

III. PROPOSED WINDOW FUNCTION

A. Covariance Matrix for the Multipath Clutter

By defining the beam steering direction as u_0 , u_T and u_R are described as

$$u_T = u_0 + \Delta u_T, \quad (9)$$

$$u_R = u_0 + \Delta u_R, \quad (10)$$

where Δu_T and Δu_R are offset angle by u_0 . From (9) and (10), $\mathbf{a}_T(u_T)$ and $\mathbf{a}_R(u_R)$ can be derived as

$$\mathbf{a}_T(u_T) = \mathbf{D}_T(u_0) \mathbf{a}_T(\Delta u_T), \quad (11)$$

$$\mathbf{a}_R(u_R) = \mathbf{D}_R(u_0) \mathbf{a}_R(\Delta u_R), \quad (12)$$

where $\mathbf{D}_T(u_0) = \text{diag}\{\mathbf{a}_T(u_0)\}$ and $\mathbf{D}_R(u_0) = \text{diag}\{\mathbf{a}_R(u_0)\}$. Thus, the MIMO steering vector is described as

$$\mathbf{a}(u_T, u_R) = \mathbf{D}(u_0) \mathbf{a}(\Delta u_T, \Delta u_R), \quad (13)$$

where $\mathbf{D}(u_0) = \mathbf{D}_T(u_0) \otimes \mathbf{D}_R(u_0)$.

We wish to have low sidelobe level where MS and SM multipath clutter is received. The MS/SM sidelobe region is indicated in gray in Fig. 2. The region is specified by parameters denoted by b_T , b_R , U_T , and U_R as seen in the figure. The covariance matrix corresponding to the MS/SM multipath clutter is given as

$$\mathbf{R}_c(u_0) = \mathbf{D}(u_0) \mathbf{R}_c \mathbf{D}^H(u_0), \quad (14)$$

where \mathbf{R}_c is

$$\mathbf{R}_c = \begin{pmatrix} \int_{-0.5b_R}^{-0.5b_T} \int_{-0.5b_T}^{0.5b_T} \mathbf{a}(\Delta u_T, \Delta u_R) \mathbf{a}^H(\Delta u_T, \Delta u_R) d\Delta u_T d\Delta u_R \\ + \int_{0.5b_R}^{U_R} \int_{-0.5b_T}^{0.5b_T} \mathbf{a}(\Delta u_T, \Delta u_R) \mathbf{a}^H(\Delta u_T, \Delta u_R) d\Delta u_T d\Delta u_R \\ + \int_{-0.5b_R}^{0.5b_R} \int_{-U_T}^{-0.5b_T} \mathbf{a}(\Delta u_T, \Delta u_R) \mathbf{a}^H(\Delta u_T, \Delta u_R) d\Delta u_T d\Delta u_R \\ + \int_{-0.5b_R}^{0.5b_R} \int_{0.5b_T}^{U_T} \mathbf{a}(\Delta u_T, \Delta u_R) \mathbf{a}^H(\Delta u_T, \Delta u_R) d\Delta u_T d\Delta u_R \end{pmatrix} \quad (15)$$

It is assumed that the average clutter power for each propagation path is the same and set unity without loss of generality.

B. Proposed Window to Mitigate the Multipath Clutter

To lower the MS/SM sidelobe level by MIMO beamforming, the loaded covariance matrix $\mathbf{R}(u_0)$ is introduced as

$$\begin{aligned} \mathbf{R}(u_0) &= \mathbf{R}_c(u_0) + \varepsilon \mathbf{I} \\ &= \mathbf{D}(u_0) \mathbf{R} \mathbf{D}^H(u_0), \end{aligned} \quad (16)$$

where $\mathbf{R} = \mathbf{R}_c + \varepsilon \mathbf{I}$, \mathbf{I} is the identity matrix and ε is the loading level. The term $\varepsilon \mathbf{I}$ behaves as an uncorrelated receiver noise covariance matrix. As the unit power level of the multipath clutter is considered in (15), setting the loading level in the range of $0 < \varepsilon \ll 1$ is typical to maintain the low-rank structure of $\mathbf{R}_c(u_0)$.

Optimum beamforming weight $\mathbf{w}_a(u_0)$, which maximizes the signal-to-interference-plus-noise ratio while mitigating the MS/SM multipath clutter is given by

$$\begin{aligned}
\mathbf{w}_a(u_0) &= \alpha_a \mathbf{R}^{-1}(u_0) \mathbf{a}(u_0, u_0) \\
&= \alpha_a \mathbf{D}(u_0) \mathbf{R}^{-1} \mathbf{D}^H(u_0) \mathbf{D}(u_0) \mathbf{a}(0, 0) \\
&= \alpha_a \mathbf{D}(u_0) \mathbf{R}^{-1} \mathbf{a}(0, 0) \\
&= \alpha_a \mathbf{D}(u_0) (\mathbf{R}^{-1} \mathbf{1}) \\
&= \alpha_a \text{diag}(\mathbf{R}^{-1} \mathbf{1}) \text{diag}(\mathbf{D}(u_0)) \\
&= \alpha_a \mathbf{T}_w \mathbf{a}(u_0, u_0)
\end{aligned} \tag{17}$$

where α_a is the normalized coefficient, $\mathbf{1}$ is all-one vector, and \mathbf{T}_w is given by

$$\mathbf{T}_w = \text{diag}(\mathbf{R}^{-1} \mathbf{1}). \tag{18}$$

\mathbf{T}_w is the diagonal matrix that behaves as a window function to $\mathbf{a}(u_0, u_0)$. Thus, the proposed window function to lower the MS/SM sidelobe level is given by $\mathbf{R}^{-1} \mathbf{1}$. The beam response $y_a(u_T, u_R)$ is given as

$$\begin{aligned}
y_a(u_T, u_R) &= \mathbf{w}_a(u_0)^H \mathbf{a}(u_T, u_R) \\
&= \alpha_a (\mathbf{a}_T^H(u_0) \otimes \mathbf{a}_R^H(u_0)) \mathbf{T}_w^H (\mathbf{a}_T(u_T) \otimes \mathbf{a}_R(u_R))
\end{aligned} \tag{19}$$

It is observed from (19) that the beam response with the proposed window is no longer separable into transmit and receive beam responses, as shown in (5). It is the generalized form of the MIMO bidirectional beam response with the window function. The beam response in (5) is a special case of that shown in (19) where the window is applied as $\mathbf{T}_w = \mathbf{T}_T \otimes \mathbf{T}_R$ such as Hamming-on-Hamming.

IV. COMPUTER SIMULATION

To evaluate the proposed window, MIMO-HFSWR with an operating frequency at 15 MHz is considered. A 32-element ULA with half-wavelength inter-element distance for both the transmit and receive functions is assumed. The beam steering direction is the boresight without loss of generality.

In Fig. 3, the MIMO bidirectional beampattern without a window function is presented. Fig. 4 shows 2-way beampattern appearing in the diagonal slice where DOA is equal to DOD for the bidirectional beampattern. The peak sidelobe level ratio (PSLR) of the slice is -26.6 dB; this is because both the transmit and receive beampatterns have the same PSLR of -13.3 dB. In Fig. 3, we observe that there is a higher sidelobe region along the horizontal and vertical axes associated with the main beam; this region corresponds to the MS/SM propagation path. The horizontal and vertical slices of the bidirectional beampattern are presented in Fig. 5. These slices are identical with the receive and transmit beampatterns with -13.3 dB PSLR, respectively. This result indicates that MS/SM multipath clutter might be received at a higher power level compared with direct-clutter.

The bidirectional beampattern shown in Fig. 3 is used for specifying the sidelobe region that one wishes to lower using the proposed window function. In this simulation, the parameter is specified as $U_R : +7.0^\circ \sim +90^\circ$, $b_T : -4.5^\circ \sim +4.5^\circ$,

$U_T = U_R$ and $b_R = b_T$; \mathbf{R}_c is calculated as per this specification. The eigenvalue distribution of \mathbf{R}_c is shown in red in Fig 6(a). It is obvious that \mathbf{R}_c has a low-rank structure; thus, the MIMO steering vector belonging to the sidelobe region span the subspace of the MIMO radar array manifold. Fig. 6(b) shows the cumulative contribution ratio of the eigenvalue of \mathbf{R}_c . In this simulation, 0.999999 of the cumulative contribution ratio is adopted to determine the loading level ε for \mathbf{R} . Specifically, when the minimum eigen-index that satisfies > 0.999999 of the ratio is selected, the corresponding eigenvalue is used as ε . Eigenvalue distribution of the loaded covariance matrix \mathbf{R} is shown in blue in Fig. 6(a).

The proposed window function is obtained using (18), and the resultant window function is presented in Fig. 7. For comparison, a conventional Hamming-on-Hamming window is presented. It is observed there is a slight difference in the behavior of these functions at the edges of these functions.

The MIMO bidirectional beampattern with the proposed window is presented in Fig. 8. Compared with no window case in Fig. 3, the main beam region is broadened on applying the proposed window. The entire sidelobe level, including the region where we wish to lower, is obviously lowered. The MIMO bidirectional beampattern with the conventional Hamming-on-Hamming window is presented in Fig. 9 to compare with Fig. 8. It is observed that the sidelobes on the horizontal and vertical axes of the proposed window case demonstrate better performance while the main beam region of both windows is approximately same. The beampatterns of the horizontal and vertical axes associated with the main beam are shown in Fig. 10 for reference.

For a detailed inspection of the performance, the diagonal slices satisfying the condition DOD = DOA are shown in Fig. 11. The top chart is a full-scale view, and the bottom chart is an enlarged view of the main beam. Mismatch loss and 3 dB beamwidth are inspected, and the results are listed in Table 1. The mismatch loss is normalized to the case involving no window. From Figs. 8 and 9, we observe that the loss and the beamwidth are nearly identical to each other. This means that the following inspection on the sidelobe performance is a fair comparison while evaluating the effect of the proposed window over the conventional Hamming-on-Hamming window.

As presented in Table 1, the PSLR of the proposed window is -42.6 dB, which is slightly better than the -41.8 dB PSLR of the conventional Hamming-on-Hamming window. In the table, integrated sidelobe level ratio (ISLR) is presented for both windows. ISLR is defined as the ratio of the total power of the sidelobe region to that of the main beam null-to-null region. The ISLR of the proposed window is -37.8 dB, which is 7.9 dB better than that of the conventional Hamming-to-Hamming window. As multipath clutter is distributed over a wide illuminated area, the ISLR performance is a more appropriate figure of merit than the PSLR in HFSWR.

The computer simulation result involves just a single example for the proposed window mentioned in this section, and the performance will be controlled by flexible parameter configuration. The performance including practical antenna issues such as mutual coupling will be investigated in the future.

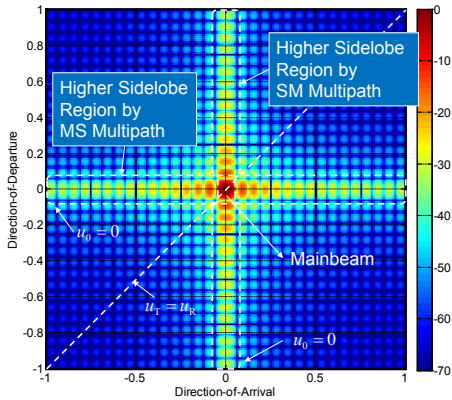
V. CONCLUDING REMARKS

In this paper, a new window function for MIMO radar beamforming to mitigate multipath clutter is proposed. The proposed window is derived by modeling unwanted echo traveling the MS/SM propagation path. The computer simulation result indicates that the proposed window has a -37.8 dB ISLR, which is 7.9 dB better than that of the conventional Hamming-on-Hamming window while maintaining comparable performance in mismatch loss, beamwidth, and PSNR. The performance of the proposed window will be controlled by flexible parameter specification.

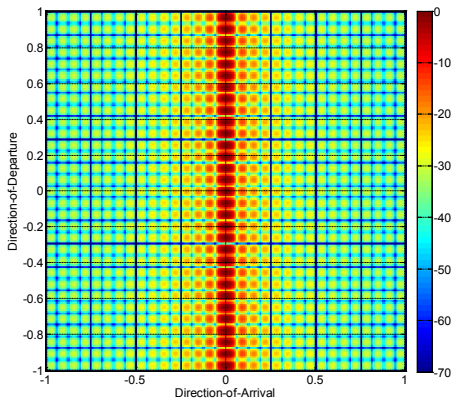
REFERENCES

- [1] D. J. Rabideau and P. Parker, "Ubiquitous MIMO multifunction digital array radar," The Thirty-Seventh Asilomar Conference on Signals, Systems & Computers, vol. 1, pp. 1057-1064, 2003.
- [2] J. Kantor and S. K. Davis, "Airborne GMTI using MIMO techniques," 2010 IEEE Radar Conference, Washington, DC, 2010, pp. 1344-1349.
- [3] F. C. Robey, S. Coumts, D. Weikle, J. C. McHarg and K. Cuomo, "MIMO radar theory and experimental results," Conference Record of the Thirty-Eighth Asilomar Conference on Signals Systems & Computers, Nov. 2004.
- [4] J. Klare and O. Saalman, "MIRA-CLE X: A new imaging MIMO-radar for multi-purpose applications," The 7th European Radar Conference, Paris, 2010, pp. 129-132.
- [5] J. O. Hinz, T. Fickenscher, A. Gupta, M. Holters and U. Zölzer, "Evaluation of time-staggered MIMO FMCW in HFSWR," 2011 12th International Radar Symposium (IRS), Leipzig, 2011, pp. 709-713.

- [6] S. M. Patole, M. Torlak, D. Wang and M. Ali, "Automotive Radars: A review of signal processing techniques," IEEE Signal Processing Magazine, vol. 34, no. 2, pp. 22-35, March 2017.
- [7] S. Anderson, "OTH radar phenomenology: signal interpretation and target characterization at HF," IEEE Aerospace and Electronic Systems Magazine, vol. 32, no. 12, pp. 4-16, December 2017.
- [8] S.J. Anderson, "Multiple scattering of HF surface waves: Implications for radar design and sea clutter interpretation," IET Radar Sonar and Navigation, vol. 4, no. 2, pp. 195-208, 2010.
- [9] S. J. Anderson and W. C. Anderson, "A MIMO technique for enhanced clutter selectivity in a multiple scattering environment: Application to HF surface wave radar," 2010 International Conference on Electromagnetics in Advanced Applications, Sydney, NSW, 2010, pp. 133-136.
- [10] Y. I. Abramovich, G. J. Frazer and B. A. Johnson, "Noncausal Adaptive Spatial Clutter Mitigation in Monostatic MIMO Radar: Fundamental Limitations," IEEE Journal of Selected Topics in Signal Processing, vol. 4, no. 1, pp. 40-54, Feb. 2010.
- [11] Y. I. Abramovich, G. J. Frazer and B. A. Johnson, "Principles of Mode-Selective MIMO OTHR," IEEE Transactions on Aerospace and Electronic Systems, vol. 49, no. 3, pp. 1839-1868, July 2013.
- [12] J. Yu and J. Krolik, "MIMO adaptive beamforming for nonseparable multipath clutter mitigation," IEEE Transactions on Aerospace and Electronic Systems, vol. 50, no. 4, pp. 2604-2618, October 2014.
- [13] F. Robey, V. Mecca, *MIMO Radar: Over The Horizon Radar Use Case*, Phased Arrays for MIMO Radar Tutorial, IEEE International Symposium on Phased Array Systems and Technology, 18 Oct. 2016, Waltham, MA.
- [14] G. J. Frazer, "Experimental results for MIMO methods applied in over-the-horizon radar," IEEE Aerospace and Electronic Systems Magazine, vol. 32, no. 12, pp. 52-69, December 2017.



(a) Thirty-two-element transmit and receive ULA



(b) Two-element sparse transmit array with 32-element receive ULA

Fig. 1. Representative MIMO bidirectional beampattern.

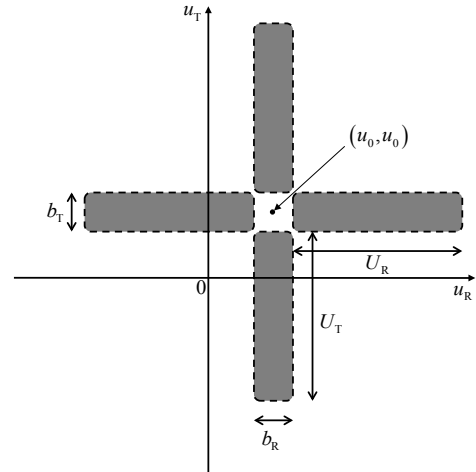


Fig. 2. Specification of the sidelobe region to be lowered.

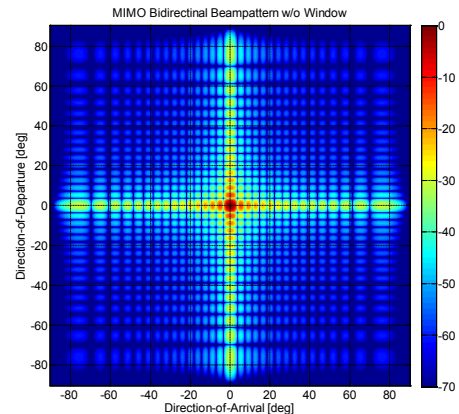


Fig. 3. MIMO bidirectional beampattern without window function.

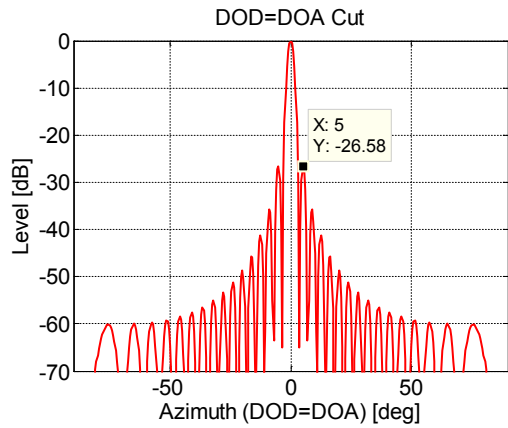
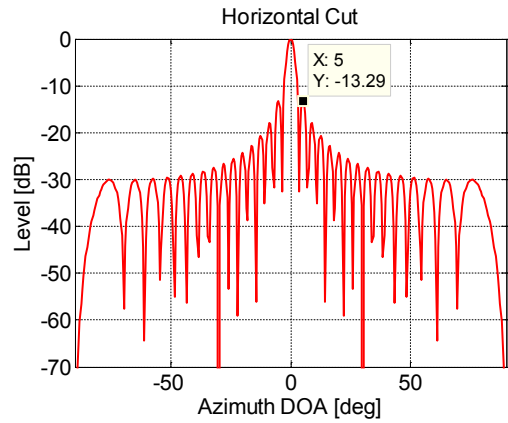
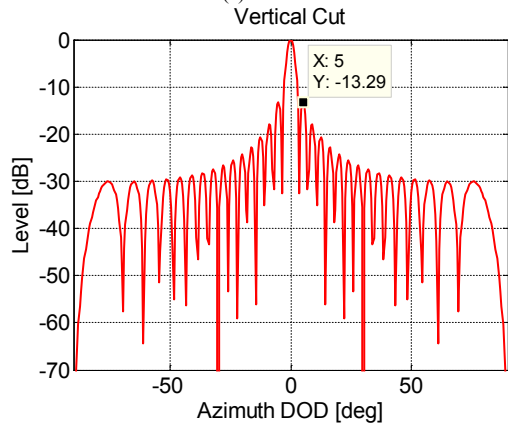


Fig. 4. Two-way beampattern or the diagonal slice satisfying the condition DOA = DOA.

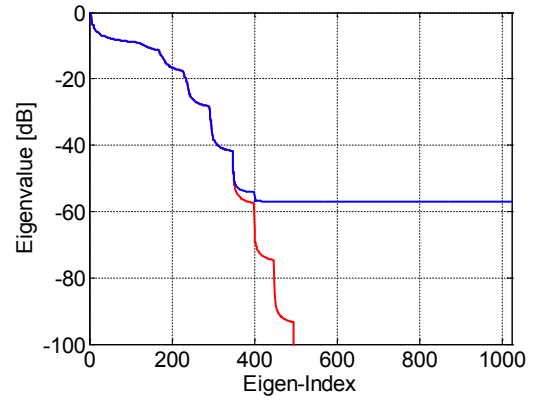


(a) DOD = 0°

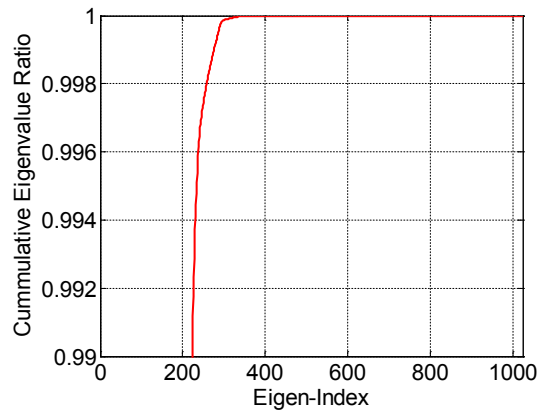


(b) DOA = 0°

Fig. 5. Slices of the MIMO bidirectional beampattern.



(a) Eigenvalue distribution of \mathbf{R}_c (red) and \mathbf{R} (blue).



(b) Cumulative contribution ratio of the eigenvalue of \mathbf{R}_c .

Fig. 6. Eigenvalue analysis of \mathbf{R}_c and \mathbf{R}

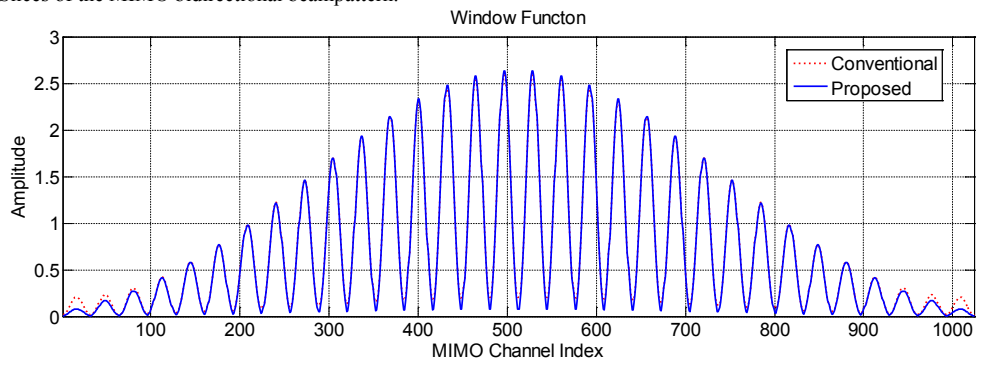


Fig. 7. Proposed and conventional Hamming-on-Hamming window functions.

TABLE I. MISMATCH LOSS AND BEAMWIDTH

	Proposed Window	Conventional Window
Missmatch loss	-3.1 dB	-2.9 dB
3 dB beamwidth	3.5 °	3.6 °
PSLR	-42.6 dB	-41.8 dB
ISLR	-37.8 dB	-29.9 dB

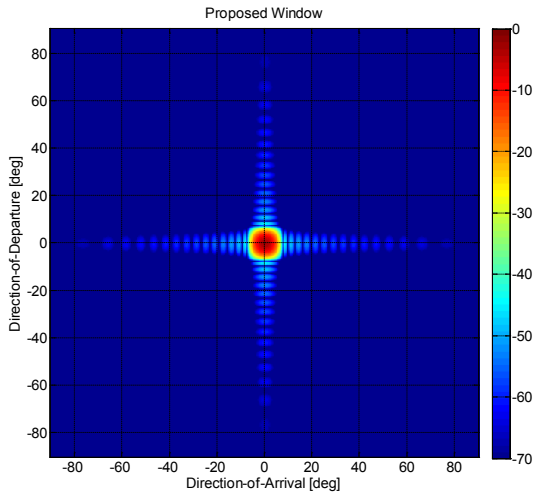


Fig. 8. The MIMO bidirectional beampattern with the proposed window.

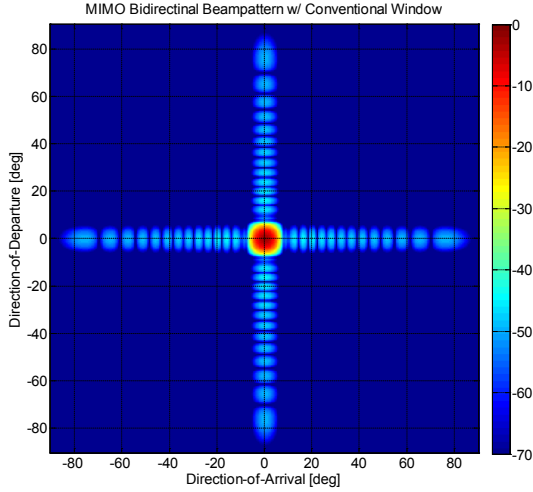
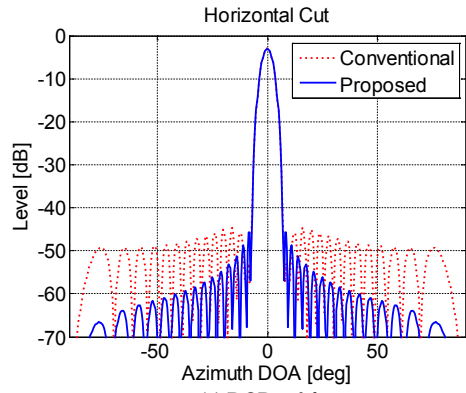
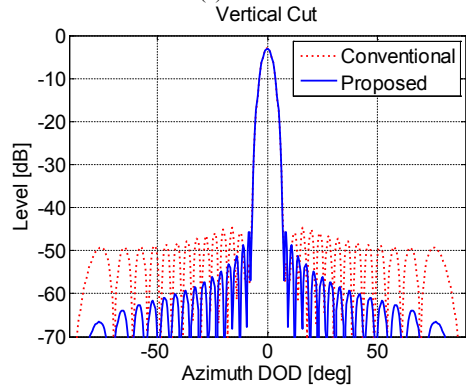


Fig. 9. The MIMO bidirectional beampattern with the conventional Hamming-on-Hamming window.

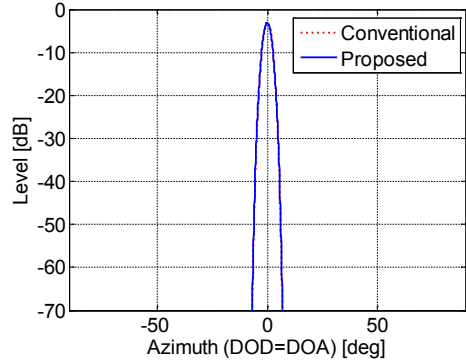


(a) DOD = 0 °

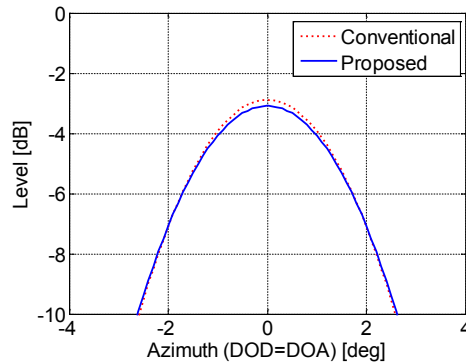


(b) DOA = 0 °

Fig. 10. Slices of the MIMO bidirectional beampattern. DOD=DOA Cut



(a) Full Scale



(b) Enlarged

Fig. 11. Two-way beampattern or the diagonal slice satisfying the condition DOA = DOA.